NeuroImage: Clinical 38 (2023) 103372

Contents lists available at ScienceDirect

NeuroImage: Clinical

journal homepage: www.elsevier.com/locate/ynicl

Spinal cord atrophy after spinal cord injury – A systematic review and meta-analysis

Carl Trolle [a,b,*], Estee Goldberg [a], Clas Linnman [a]

[a] Spaulding Rehabilitation Hospital, Department of Physical Medicine and Rehabilitation, Harvard Medical School, Boston, MA, USA
[b] Department of Medical Sciences, Rehabilitation Medicine, Uppsala University, Uppsala, Sweden

ARTICLE INFO

Keywords:
MRI
Neurotrauma
DTI
Rehabilitation
Biomarker

ABSTRACT

Cervical spinal cord atrophy occurs after spinal cord injury. The atrophy and how level of injury affects atrophy differs between studies. A systematic review and metaanalysis were done after systematic searches of PubMed, CINAHL, APA PsycInfo and Web of Science. English language original studies analyzing MRI cervical spinal cord cross-sectional area in adults with spinal cord injury were included. Atrophy and correlation between injury level and atrophy were estimated with random-effects models, standardized mean differences, and 95% confidence intervals. 24 studies were identified. 13/24 studies had low risk of bias. Cord atrophy meta-analysis of 18 articles corresponded to a standardized mean difference of -1.48 (95% CI -1.78 to -1.19) with moderate to large inter-study heterogeneity. Logarithmic time since injury influenced heterogeneity. Longitudinal atrophy was best described by a logarithmic model, indicating that rate of spinal atrophy decreases over time. Meta-correlation of eight studies indicated more severe atrophy in more rostral injuries (0.41, 95% CI 0.20-0.59). Larger and preferably longitudinal studies, data sharing, and standardized protocols are warranted.

1. Introduction

After spinal cord injury (SCI) there is rapid and progressive spinal cord atrophy (Azzarito et al., 2020; David et al., 2021; Freund et al., 2013; Ziegler et al., 2018). The primary injury leads to spinal cord tissue damage, which is exacerbated by a neuro-immune response. Pro-inflammatory cytokines are released from invading monocyte-derived macrophages resulting in neuronal apoptosis and the physical contact between monocyte-derived macrophages and dystrophic axons initiates secondary axonal retraction (Oyinbo, 2011; Van Broeckhoven et al., 2021). Rostral to the injury, spinal atrophy appears initially higher in white matter whereas below the level of injury (LoI), grey and white matter atrophy progress similarly (David et al., 2021). White matter atrophy has been attributed to axonal degeneration and demyelination while grey matter atrophy may stem from transsynaptic neuro-degeneration (Huber et al., 2018).

A common MRI-measurement to assess spinal cord atrophy is cross-sectional cervical spinal cord area (cSC CSA) (Cohen-Adad et al., 2011; Freund et al., 2010; Schmit and Cole, 2004). Typically, T1-MPRAGE (Freund et al., 2013), T2- (Cohen-Adad et al., 2011) or T2*-sequences are used (David et al., 2022). Smaller cSC CSA has been associated with poorer motor and sensory function, less functional independence, as well as neuropathic pain in persons with paraplegia (Freund et al., 2013; Hou et al., 2016; Jutzeler et al., 2016; Lundell et al., 2011; Ziegler et al., 2018). Similarly, dorsal horn and ventral horn atrophy are associated with pinprick score and motor score respectively (Huber et al., 2018).

Despite the consistency in reports confirming spinal cord atrophy after SCI, there are important interstudy differences in imaging techniques and image analysis (Cohen-Adad et al., 2011; Ohn et al., 2013; Schmit and Cole, 2004). Similarly, intra- and interstudy differences exist in study participant factors known to influence cSC CSA, such as sex, time since injury (TSI), age, and injury severity (David et al., 2021; Freund et al., 2013; Papinutto et al., 2015; Seif et al., 2020; Solstrand Dahlberg et al., 2020; Ziegler et al., 2018). Results are mixed on whether the level of injury affects spinal cord atrophy: greater cord atrophy has been reported in persons with tetraplegia compared to persons with paraplegia (Jutzeler et al., 2016) and one study (Lundell et al., 2011) described a modest correlation between LoI and atrophy. One study, however, did not find any correlation between cSC CSA and LoI (Sangari et al., 2019).

The aims of this systematic review and meta-analysis were to

* Corresponding author at: Spaulding Neuroimaging Laboratory, 300 First avenue, Charlestown, MA 02129, USA.
E-mail addresses: ctrolle@partners.org, carl.trolle@neuro.uu.se (C. Trolle), clinnman@partners.org (C. Linnman).

https://doi.org/10.1016/j.nicl.2023.103372
Received 30 November 2022; Received in revised form 12 February 2023; Accepted 6 March 2023
Available online 10 March 2023

determine the magnitude, effect size, and consistency of spinal cord atrophy across studies. The effect of LoI and TSI on cSC CSA were also examined and the associations between cSC CSA and functional outcomes were described.

2. Methods

2.1. Inclusion criteria

The Preferred Reporting Items for Systematic Reviews and Meta-Analyses (PRISMA) guidelines were followed (Page et al., 2021). The PICO-criteria were stipulated as:

Population – adult persons with spinal cord injury (PwSCI). Degenerative spine disorders were not included, nor cauda equina (Awai and Curt, 2015) or where MRI images were obtained at admission or the early days after admission (Rüegg et al., 2015; Song et al., 2009). No year limit was used for the searches.

Investigated test result – structural MRI or diffusion tensor imaging (DTI).

Control – healthy controls. Only studies presenting data from MRI or DTI cSC CSA in PwSCI and controls were included in cSC CSA meta-analysis. Articles without controls were included if they provided data for use in longitudinal, regression or correlational analyses.

Outcome – cSC CSA. Only English language articles were included.

This study was not registered in PROSPERO. A review protocol was not prepared.

2.2. Search strategies

A PubMed search strategy was developed through an iterative process and validated against a previously selected set of eligible studies reporting cSC CSA that were already known by the study team (Azzarito et al., 2020; David et al., 2021; Freund et al., 2013; Hou et al., 2016; Hug et al., 2021; Jutzeler et al., 2016; Lundell et al., 2011; Ohn et al., 2013; Sangari et al., 2019; Seif et al., 2018, 2020; Ziegler et al., 2018). Once a PubMed search strategy capable of identifying the validation set was established, the search was expanded to Web of Science, CINAHL and APA PsycInfo databases. CINAHL and APA PsycInfo were searched simultaneously through the EBSCOhost Research Database, initially between January 31st and February 2nd, 2022.

For PubMed (initial search conducted January 31st, 2022), the following strategy was used:

Spinal cord injury [MeSH Terms] AND humans [MeSH Terms] AND (“MRI” OR magnetic resonance imaging OR diffusion tensor imaging OR “DTI”) AND (“cross-section” OR “spinal cord area” OR “measur*” OR atroph*).

For Web of Science (February 1st-2nd 2022), the following search terms (separated for clarity by “|”) were used: TS= (“spinal cord injury”) OR TS= (“SCI”) | MRI (Topic) or magnetic resonance imaging (Topic) or DTI (Topic) or diffusion tensor imaging (Topic) | humans (Topic) | cross-sectional (Topic) or spinal cord area (Topic) or measur* (Topic) or atroph* (Topic). Search terms were combined using the Boolean operator “AND”.

For CINAHL and APA PsycInfo (February 2nd, 2022), a similar combination of search terms was used: (TX “spinal cord injuries”) (TX humans) (TX magnetic resonance imaging OR TX mri OR TX diffusion tensor imaging OR TX dti) (TX cross-section OR TX spinal cord area OR TX measur* OR TX atroph*), these search terms were likewise combined using the Boolean operator “AND”.

After these search processes, the study team was informed through personal correspondence about a recent article which the search strategies did not identify (David et al., 2022). Searches were updated on June 14th, 2022, identifying the one additional study not found during previous database searches (David et al., 2022).

All studies were screened for eligibility by title and abstract by one author (CT). Articles identified were subjected to a full-text screening by the same author. Titles of all references in included articles were examined for additional items, which led to the identification of one more article (Wyss et al., 2019).

2.3. Unique participants

If cSC CSA-data from the PwSCI study population had been reported elsewhere or where we did not receive information stating the contrary, the study with highest number of PwSCI participants or the study from which we were able to retrieve the most data was analyzed (Azzarito et al., 2021; Freund et al., 2010, 2011a, 2012a, 2012b; Grabher et al., 2015; Huber et al., 2018; Ziegler et al., 2018). Studies with overlapping PwSCI populations were included in the systematic review if they provided different and/or additional measurements. If deemed necessary, the corresponding author was contacted through e-mail for clarification. Unique individuals from overlapping study populations were identified by comparing participant demographics; if there were any discrepancies between demographical data, the participant was considered to be unique.

2.4. Data collection and imputations

Data was collected by one author (CT) using a data collection template. Data entries were cross-checked by another author (EG). Deduplication was performed in Microsoft Excel (version 16.55 – 16.61) by comparing PubMed-ID (PMID) or other article metadata if PMID was not available.

In articles where values were given for subgroups of PwSCI, a pooled mean value and standard deviation was calculated for all PwSCI if possible. If means for demographic parameters (e.g., age, TSI) were not presented, this was calculated using individual subject data if possible.

If cSC CSA at several separate spinal levels were presented, the C2-level was used for cSC CSA meta-analysis (Azzarito et al., 2020). If sensory and motor LoI were reported, the most cephalad/rostral level was used. For one longitudinal study, cSC CSA was averaged across the different measured time points to decrease study weight (Freund et al., 2013). For another longitudinal study, 2-month cSC CSA-values were used due to data availability reasons (David et al., 2021).

In one article (Mesbah et al., 2021) presenting graphical cSC CSA-data, an averaged mean cSC CSA was extracted from supplemented data provided in the article by averaging values from the two observers. A similar data extraction was conducted on one further article (Kikkert et al., 2021). For both articles, cSC CSA, AIS, LoI and demographic parameters were retrieved. When necessary and possible, manual data extraction from study graphs using the software WebPlotDigitizer (Rohatgi, 2021) was performed to retrieve additional data points.

One study (Wyss et al., 2019) provided only the % difference and statistical tests of cSC CSA between controls and PwSCI, but graphical information on cSC CSA of the PwSCI participants. Using the available data (% difference and p-values), we estimated control cSC CSA using an iterative simulation with random noise inserted until results matched those reported in the publication. For another study in which only control median cSC CSA and quartiles were available (Freund et al., 2011b), control mean cSC CSA and standard deviation were approximated using inbuilt functions of the R *meta* package version 5.5-0 (Balduzzi et al., 2019). In a study where individual cSC CSA-values were available but not all individual demographical parameters (David et al., 2021), these missing parameters (TSI, age) were estimated using mean imputation.

Means and standard deviations were, if not provided, calculated in Microsoft Excel (version 16.55 – 16.61). CT and CL conducted statistical analyses.

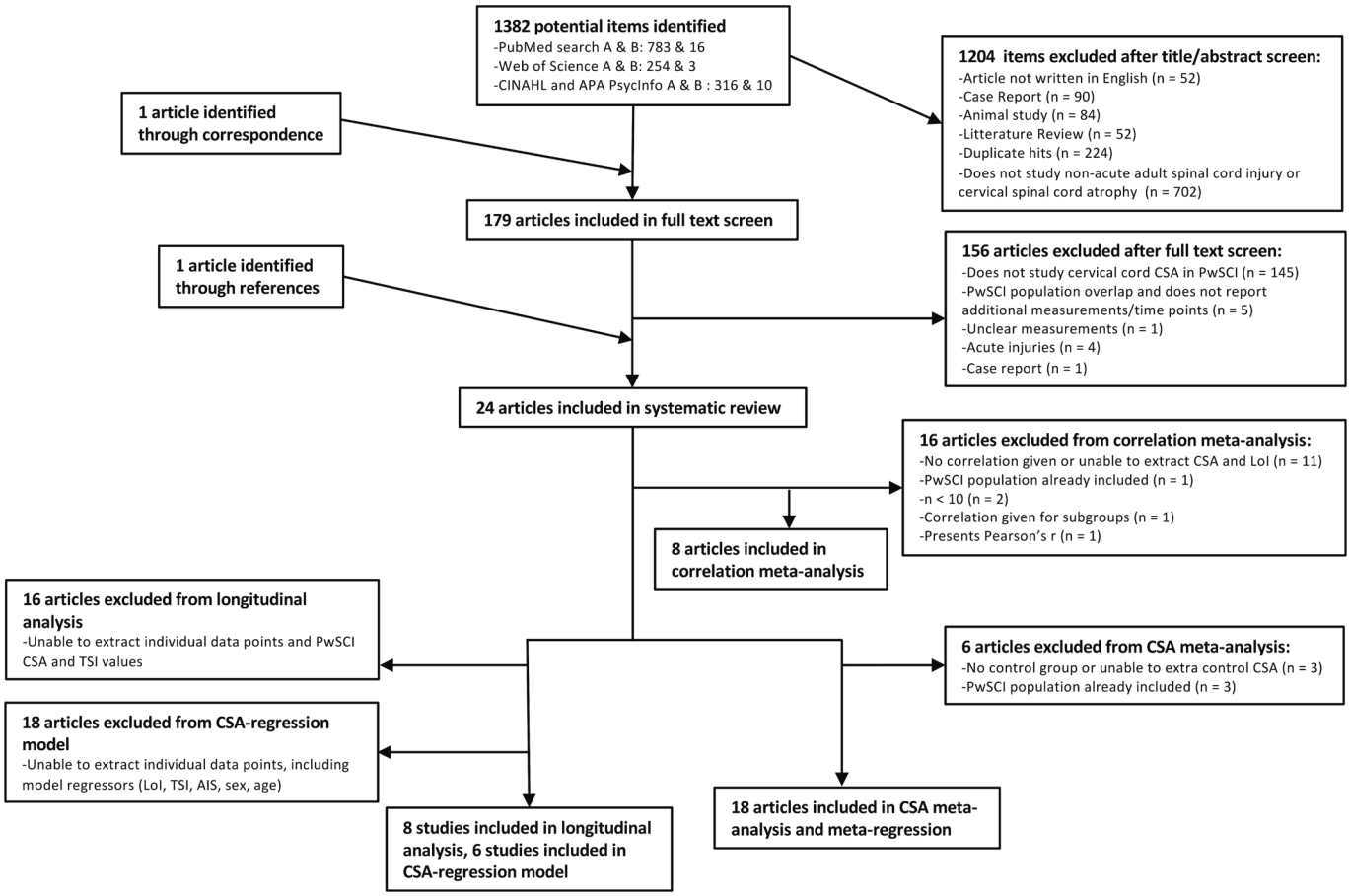

Fig. 1. PRISMA (Preferred Reporting Items for Systematic Reviews and Meta-Analyses) flow diagram depicting the literature selection process. A represents the number of initial hits and B represents the number of non-duplicate new hits retrieved with the final search.

2.5. Statistical methods

2.5.1. Meta-analysis and meta-regression

A random effects model was used for meta-analyses with heterogeneity variance calculated using the restricted maximum likelihood estimator (REML) (Viechtbauer, 2005). A small sample bias corrected standardized mean difference was used (Hedges' g), with exact formulae. Study weights were determined using the inverse variance method. A p-value < 0.05 was considered statistically significant. Heterogeneity was explored further using meta-regression.

2.5.2. Meta-correlation

For meta-correlation between cSC CSA and LoI, coefficients were retrieved from two articles (Jutzeler et al., 2016; Lundell et al., 2011). For three articles, corresponding Spearman's ρ were calculated manually based on supplementary information (Kikkert et al., 2021; Mesbah et al., 2021) or through information provided by study authors through correspondence (David et al., 2021). In four articles (Azzarito et al., 2020; Freund et al., 2013, 2011b; Pfyffer et al., 2020), cSC CSA and corresponding LoI was retrieved using WebPlotDigitizer (Rohatgi, 2021) after which Spearman's ρ was calculated. For one of these articles presenting longitudinal data, an averaged cSC CSA per participant was calculated by averaging cSC CSA at the different studied timepoints (Freund et al., 2013). Articles with more complex correlation analyses or models, or in which correlations were presented for subgroups of PwSCI, were not included (Sangari et al., 2019; Ziegler et al., 2018) unless individual cSC CSA and corresponding LoI could be extracted (Azzarito et al., 2020). For Azzarito et al (2020), the correlation between level and C2 cSC CSA was not available, rather, the correlation between level and average cSC CSA for C1-C4 was provided. As the C1-C4 average cSC CSA is a reasonable estimate of C2 cSC CSA, these datapoints were included in the meta-correlation.

Studies with $n < 10$ were not included in the meta-correlation. Only articles with Spearman's ρ were included in the meta-correlation using Fisher's z_r-transformation (Sheshkin, 2000). To avoid including articles with different measures of correlation in the analysis, one article presenting Pearson's r (Lundell et al., 2011) was excluded following sensitivity analysis. Similar to the cSC CSA meta-analysis, a random effects model was used and heterogeneity variance calculated using REML (Viechtbauer, 2005). Study weights were determined using the inverse variance method. A p-value < 0.05 was considered statistically significant.

2.5.3. Longitudinal atrophy model

Data points from studies with available individual cSC CSA and TSI values were used. Models were fitted using either TSI or natural logarithm TSI (lnTSI) as regressor. Model selection was done using the Akaike Information Criteria (AIC). A p-value < 0.05 was considered statistically significant.

2.5.4. Multiple regression

Multiple regression was conducted using LoI as a discrete variable. AIS-categories, sex, and MRI-contrast were re-coded as dummy variables. A p-value < 0.05 was considered statistically significant.

2.5.5. Risk of bias assessment

Risk of bias (RoB) was assessed in all included articles. The core criteria from a previously published RoB-tool were used with

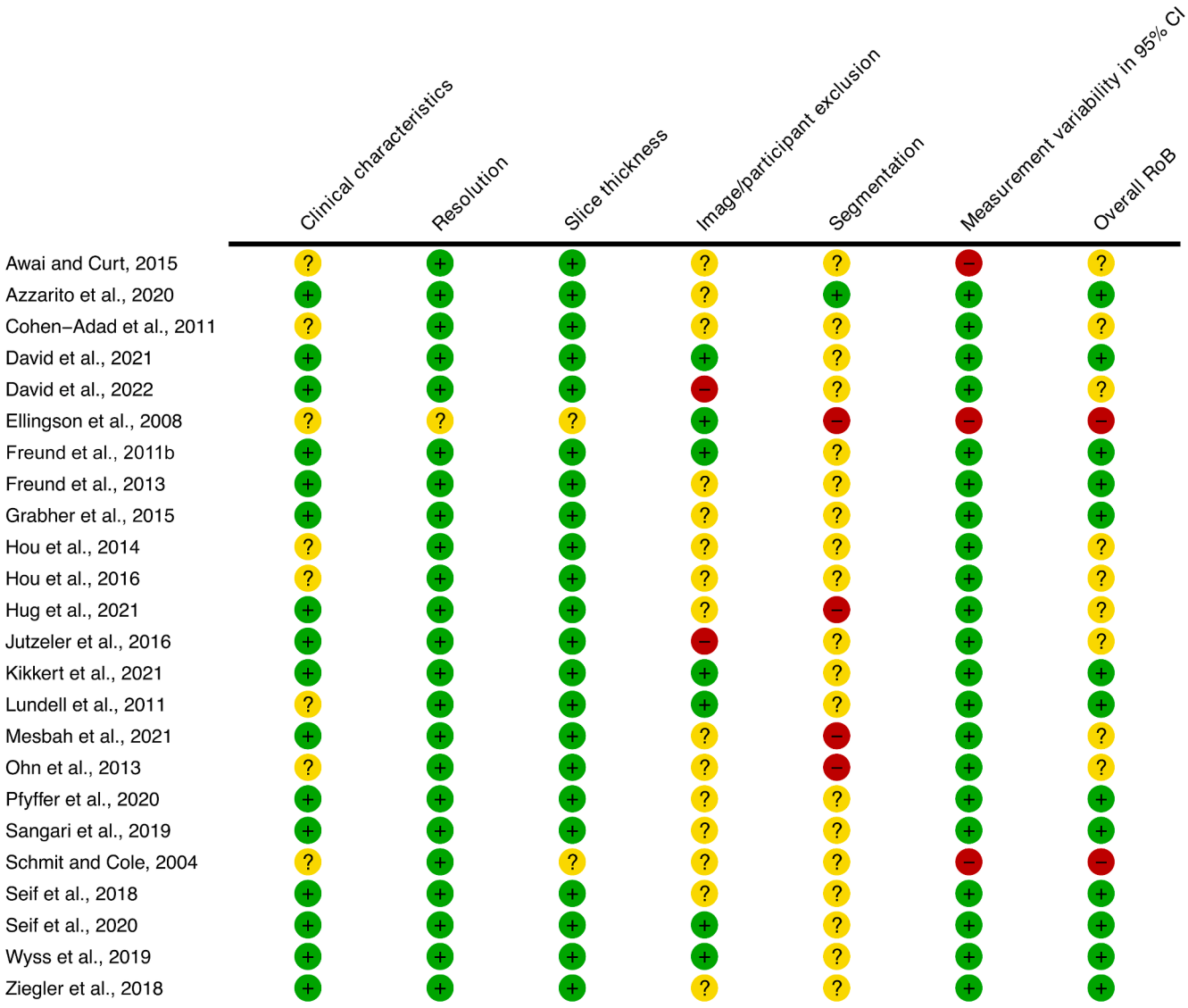

Fig. 2. Risk of Bias (RoB) plot. Circles are colour coded with green indicating low RoB, yellow indicating some concerns and red indicating a high RoB. The symbols "+", "?" and "-" indicate the same RoB-grades as the colours. (For interpretation of the references to colour in this figure legend, the reader is referred to the web version of this article.)

modifications. In the "*Study Design, Clinical Characteristics*"-criterion (Casserly et al., 2018), the categories "*multiple sclerosis disease subtype*","*expanded disability status scale*", "*disease modifying treatment*" and "*disease duration*" were removed. Instead, corresponding *American Spinal Injury Association Impairment Scale* (AIS), neurological LoI and time since injury (TSI), age, and sex were added. RoB was assessed separately by two authors (CL and CT). Disagreements were resolved through discussion. Lower imaging resolution was deemed as increasing RoB. Articles not specifying number of excluded participants or images were automatically allocated 2 RoB points. Each RoB-criterion was allocated 1–3 points. A summary score of 6–8 was considered as low RoB, 9–11 as some concerns, and 12 points or above as high RoB. The final RoB-criteria were (for 1, 2, and 3 points respectively):

Clinical characteristics: None missing, 1 or 2 missing, >2 missing.
Resolution: <1.5x1.5 mm, 1.5x1.5 mm, > 1.5x1.5 mm:
Slice thickness: <5mm, 5 mm, >5mm.
Image/participant exclusion: <3%, 3–5%, >5%.
Segmentation: automated, semiautomated, manual.
Measurement variability in 95% CI: <20%, 20%, >20% CI.

2.5.6. Software

Meta-analysis of standardized mean difference (SMD) and mean difference, meta-regression, X^2, longitudinal atrophy analysis, multiple regression and meta-correlation were calculated using R (version 4.1.2) (Harrer et al., 2021; R Core Team, 2021) with R studio (version 2021.9.1.372) (RStudio Team, 2021). Different R-packages were used to obtain presented graphs and to facilitate data management (Kassambara, 2020; Rudis et al., 2017; Slowikowski, 2021; Wickham, 2016, p. 2; Wickham and Bryan, 2019).

3. Results

3.1. Study and demographical data

A total of 1383 study abstracts were screened with publication years from 1985 to 2022. After abstract and full text screening, 23 articles were identified, and their references searched which identified one additional article (Wyss et al., 2019). Of the 24 articles, 18 (Awai and Curt, 2015; Azzarito et al., 2020; Cohen-Adad et al., 2011; David et al., 2021, 2022; Ellingson et al., 2008; Freund et al., 2011b; Hou et al., 2016, 2014; Hug et al., 2021; Jutzeler et al., 2016; Lundell et al., 2011; Ohn

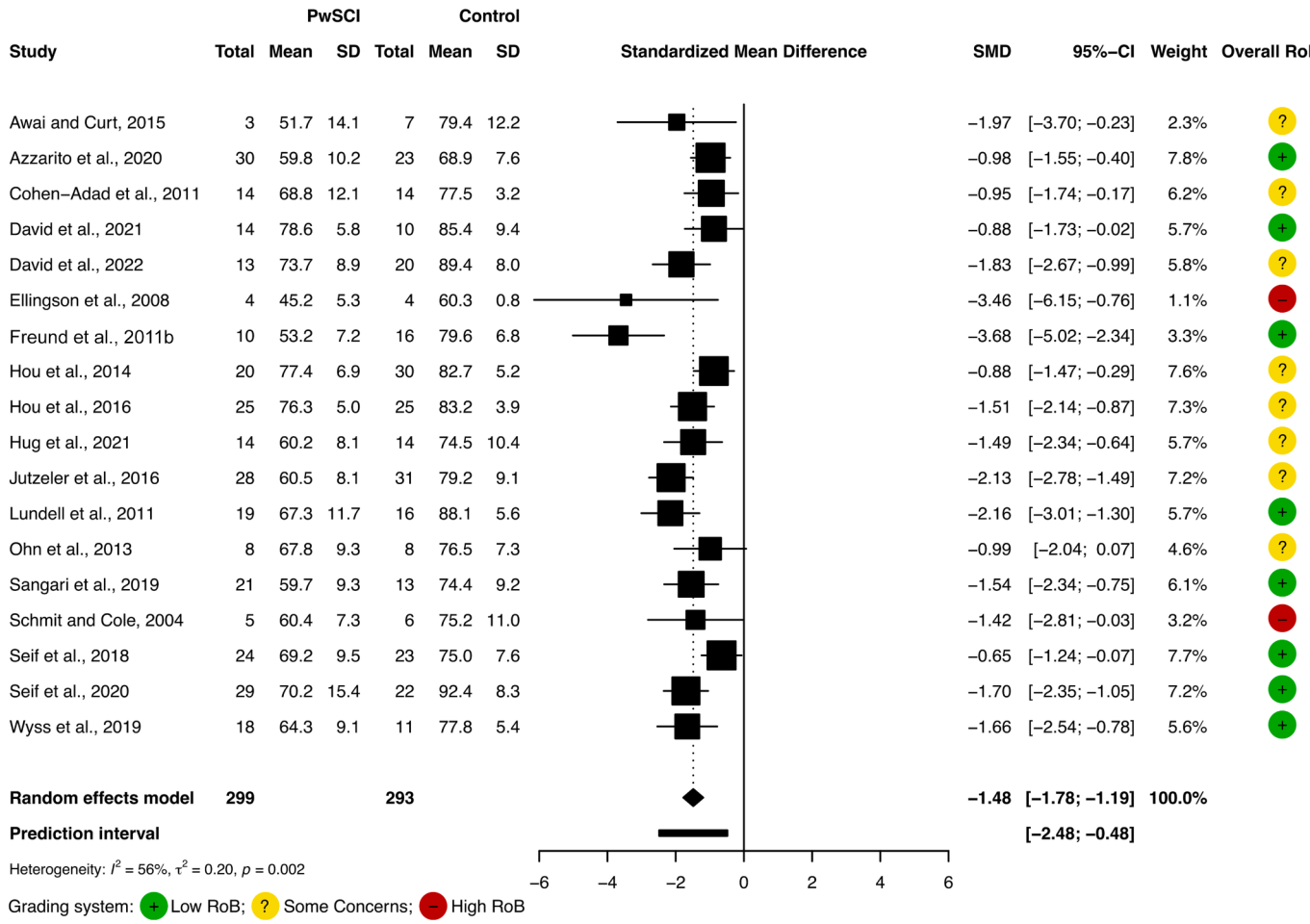

Fig. 3. Cervical spinal cord cross-sectional area atrophy (cSC CSA) meta-analysis.

et al., 2013; Sangari et al., 2019; Schmit and Cole, 2004; Seif et al., 2020, 2018; Wyss et al., 2019) were included in the cSC CSA meta-analysis and eight were included in the longitudinal analysis (Awai and Curt, 2015; David et al., 2021; Freund et al., 2013, 2011b; Kikkert et al., 2021; Mesbah et al., 2021; Pfyffer et al., 2020; Schmit and Cole, 2004). Six studies (David et al., 2021; Freund et al., 2013, 2011b; Kikkert et al., 2021; Mesbah et al., 2021; Pfyffer et al., 2020) were included in the multiple regression. Eight studies were used for meta-correlation between cSC CSA and LoI (Azzarito et al., 2020; David et al., 2021; Freund et al., 2013, 2011b; Jutzeler et al., 2016; Kikkert et al., 2021; Mesbah et al., 2021; Pfyffer et al., 2020) (Fig. 1).

A full RoB-assessment for all articles is presented in Fig. 2. A summary RoB-assessment is presented in Fig. 3 and Fig. 6 for articles included in cSC CSA meta-analysis and cSC CSA-LoI meta-correlation. Two studies (Ellingson et al., 2008; Schmit and Cole, 2004) of 24 were assessed as having a high RoB whereas nine (Awai and Curt, 2015; Cohen-Adad et al., 2011; David et al., 2022; Hou et al., 2016, 2014; Hug et al., 2021; Jutzeler et al., 2016; Mesbah et al., 2021; Ohn et al., 2013) were judged to have some concerns.

A total of 397 cSC CSA values were contributed from 352 PwSCI. At least 77.6 % (308/397) of PwSCI cSC CSA-values were identifiable as stemming from men and at least 14.9% (59/397) were from women. There were more women cSC CSA-values in control-groups than in PwSCI-groups ($X^2 = 16.1$, $p < 0.0001$). Mean TSI ranged from 0.1 to 25 years. Traumatic (≥73.0%) and non-traumatic SCI (≥3.7%) were included. All AIS categories (A ≥ 30.4%, B ≥ 14.2%, C ≥ 9.7%, D ≥ 31.8%, and E ≥ 0.6%) were represented in the study population. LoI ranged from C1 to S2 (cervical LoI ≥ 55.4%, thoracic LoI ≥ 27.6%, lumbar LoI ≥ 2.3%, and sacral LoI ≥ 0.3%). Several studies reported neurological LoI as per the International Standards for Neurological Classification of Spinal Cord Injury assessment (The American Spinal Injury Association, 2019). In some instances, LoI was determined through MRI-assessment (Cohen-Adad et al., 2011), motor level only (Freund et al., 2011b; Hou et al., 2016) or not provided. Demographics are further described in Table 1.

T1 was the most common contrast (11/24) followed by T2 (8/24), T2* (3/24), and DTI (2/24). Field strength was commonly 3 T, only 3/24 studies used 1.5 T. Image analysis was conducted using manual, semi-automated or automated methods. Semiautomated analysis was the most frequent (Table 2).

3.2. Meta-analysis of cSC CSA

Meta-analysis of cSC CSA revealed a SMD corresponding to −1.48 (95% CI −1.78 to −1.19) with smaller cSC CSA in PwSCI compared to controls (mean difference −13.5 mm^2; 95% CI −16.6 to −10.5 mm^2). Moderate-to-large heterogeneity may be present (Fig. 3). No study reported a larger cSC CSA in PwSCI than controls, but not all studies found a significantly smaller cSC CSA in PwSCI than in controls (Hou et al., 2014; Ohn et al., 2013).

3.3. Meta-regression

Heterogeneity was further explored using meta-regression (Fig. 4). Since spinal cord atrophy progresses after injury, TSI or lnTSI were included as predictors (David et al., 2021; Freund et al., 2013; Ziegler et al., 2018). Of the two, we only found the lnTSI-model to be explanatory ($p = 0.0035$ lnTSI versus $p = 0.053$ TSI) indicating that 60.7% of

Table 1
Study Demographics.

	Controls		PwSCI				
Study (first author) and year	N (women)	Age (SD)	N (women)	Age (SD)	TSI in years (SD)	AIS	LoI
Awai and Curt, 2015	7 (1)	45 (8)	3 (1)[s]	56 (3)	24.7 (5.1)	Na	T3-T7
Azzarito et al., 2020	23 (10)	37 (12)	30 (3)	45 (17)	3.0 (5.5)	A-E	C1-L3
Cohen-Adad et al., 2011	14 (5)	45 (17)	14 (3)	45 (14)	25 (35)	A-D	C3-C6[r]
David et al., 2021	10 (3)	45 (19)	14 (3)[§]	50 (16)	0.2 (0.1)	A-D	C2-L1
David et al., 2022	20 (4)	43 (15)	13 (0)	49 (13)	5.9 (5.1)	C-E	C2-C1
Ellingson et al., 2008	4 (Na)	29 (6)	4 (Na)	42 (16)	13 (12.8)	A-C	C5-T12
Freund et al., 2011b	16 (Na)	39 (15)	10 (0)	47 (11)	14.6 (6.9)	A-D	C5-C8[m]
Freund et al., 2013	18 (6)	35 (9)	13 (1)[long]	47 (20)	0.1 (0.1)	A, B, D	C4-T12
Grabher et al., 2015	18 (6)	34 (10)	14 (1)	46 (20)	0.1 (0.1)	A, B, D	C4-T12
Hou et al., 2014	30 (13)	35 (9)	20 (9)	36 (6)	0.2 (0.1)	Na	Na
Hou et al., 2016	25 (10)	37 (9)	25 (11)	37 (13)	0.2 (0.1)	A-D	C5-T12[m]
Hug et al., 2021	14 (3)	46 (16)	14 (3)	55 (13)	19.5 (19.1)	A	C3-T10
Jutzeler et al., 2016	31 (8)	42 (10)	28 (2)	46 (12)	12.5 (8.2)	A-D	C2-L3
Kikkert et al., 2021	18 (1)	56 (15)	14 (1)	55 (13)	12.1 (11.4)	A, C, D	C2-C7
Lundell et al., 2011	16 (1)	39 (14)	19 (1)	46 (12)	13 (Na)	A, D	C, T, L[||]
Mesbah et al., 2021	0	Na	19 (5)	32 (10)	6.5 (3.5)	A, B	C3-T4
Ohn et al., 2013	8 (0)	43 (4)	8 (0)	42 (5)	2.7 (4.6)	C, D, Unknown	Na[e]
Pfyffer et al., 2020	21 (3)	46 (11)	23 (Na)	51 (11)	13.5 (9.7)	A-D	C2-L1
Sangari et al., 2019	13 (Na)	Na	21 (4)	42 (14)	11.6 (10.3)	A, B	C2-T12
Schmit and Cole, 2004	6 (Na)	Na	5 (Na)	Na	9.1 (8.6)	A-C	C4-C7
Seif et al., 2018	23 (10)	36 (11)	24 (5)	50 (20)	0.1 (0.1)	A-D	C3-S2
Seif et al., 2020	22 (8)	41 (11)	29 (5)	47 (20)	7.3 (8.0)	A-D	C1-C8
Wyss et al., 2019	11 (0)	45 median	18 (0)	50 (10)	13.9 (10.1)	A-D	C2-L1
Ziegler et al., 2018	18 (7)	34 (10)	15 (1)[long]	48 (20)	0.1 (0.1)	A, B, D	C4-T12
Total number of cSC CSA-values	*386 (99); known women to men ratio = 0.4*		*397 (59); known women to men ratio = 0.2*				
Average sample size (n)	*16*		*17*				
Known age range		*29 – 56*		*32 – 56*			
TSI range					*0.1–25*		

Overview of demographic characteristics of included studies. Values are for persons with spinal cord injury (PwSCI) contributing cross-sectional cervical spinal cord area (cSC CSA) measurements. The "known women to men ratio" was calculated for studies where we were able to specify participant sex. TSI = Time Since Injury. AIS = American Spinal Injury Association Impairment Scale. LoI = Level of Injury. Na = Not available. [s] = Syrinx-participants. [r] = Radiological level of lesion. § = Longitudinal study. cSC CSA from 14 participants were used in the cSC CSA meta-analysis, longitudinal analysis, linear model and meta-correlation analysis. [long] = Longitudinal study, all participants are included in the demographics table. [m] = LoI determined by motor level only. || = LoI specified as cervical, thoracic, or lumbar. [e] = Electrical spinal cord injury.

the differences in true effect sizes is attributable to lnTSI. The model has the following equation: SMD = cSC CSA standardized mean difference = −1.27 – (0.178*ln(years after injury).

3.4. Longitudinal atrophy model

A lnTSI-model and a TSI-model was fitted to estimate the trajectory of cSC CSA atrophy over time using individual data points extracted from eight studies (Awai and Curt, 2015; David et al., 2021; Freund et al., 2013, 2011b; Kikkert et al., 2021; Mesbah et al., 2021; Pfyffer et al., 2020; Schmit and Cole, 2004) (Fig. 5). Both models were significant ($p < 0.0001$ and $p = 0.0001$) but the lnTSI-model had a better fit per the AIC-values (752 versus 788). The respective model equations were cSC CSA $mm^2 = 67.8 – (4.56*\ln(\text{years after injury}))$ and cSC CSA = 66.9 – (0.51*years after injury).

3.5. Meta-correlation

A moderate correlation was found between LoI and cSC CSA (Fig. 6) when analyzing Spearman's ρ, suggesting that cSC CSA atrophy is greater with more rostral injuries. Inclusion of the article presenting Pearson's r (Lundell et al., 2011) resulted in a slightly higher correlation (0.43, 95% CI 0.25–0.59). Given that data points from four studies (Azzarito et al., 2020; Freund et al., 2013, 2011b; Pfyffer et al., 2020) were extracted by study authors, the meta-correlation was repeated excluding these four studies; a slightly weaker correlation was found (0.37, 95% CI 0.05 – 0.62). No study reported a larger cSC CSA in more rostral injuries. Heterogeneity was smaller in the eight study meta-correlation than in the meta-analysis.

3.6. Multiple regression

As both lnTSI and LoI influenced cSC CSA, a linear model was created with additional covariates reported to affect cSC CSA (age, AIS-category, and sex), as well as MRI-contrast. Covariates were extracted where possible and the final model included data from six studies, totaling 88 PwSCI. lnTSI, LoI and sex all contributed to cSC CSA (overall model: adjusted $R^2 = 0.51$, $F(8, 79) = 12.17$, $p < 0.0001$). For lnTSI, LoI, and sex, the β-values were −0.53, 0.29, and −0.20 with p-values corresponding to < 0.0001, 0.0008, and 0.014 respectively.

3.7. Associations between cSC CSA and functional outcomes

Most studies analyzed other parameters in addition to cSC CSA, such as functional outcomes, and motor and sensory scores. Although cSC CSA atrophy progresses with time, articles with a longitudinal design unanimously reported an improvement in PwSCI Spinal Cord Independence Measure (SCIM)-scores (David et al., 2021; Freund et al., 2013; Ziegler et al., 2018). The recovery trajectory after SCI appears to be steeper the first six months after injury and better SCIM-scores at 12 months post injury are associated with reduced loss of cSC CSA between baseline (35.5 days after injury) and 12 months post injury (Pearson's r = 0.77) (Freund et al., 2013). Further, PwSCI with greater mean cord area had better SCIM-scores as reported in one study ($r^2 = 0.215$)

Table 2
Study imaging parameters.

Study	Field strength	Scanner	Contrast	Slice thickness	In-plane resolution	cSC CSA-level	Image analysis
Awai and Curt, 2015	3 T	Siemens Magnetom Verio	T2	3 mm	1.6x2mm	C2, C2/C3	Jim 6.0/Semi, ASM (Horsfield et al., 2010)
Azzarito et al., 2020	3 T	Siemens Magnetom SkyraFit and Verio	T1-3D MPRAGE	1 mm	1x1mm	C1, C2, C3, C4	Spinal cord toolbox/Auto
Cohen-Adad et al., 2011	3 T	Siemens TIM Trio	T2-SPACE	0.9 mm	0.9x0.9 mm	C1-C2	Semi, Losseff (Losseff et al., 1996)
David et al., 2021	3 T	Siemens SkyraFit	T2*-3D MEDIC	2.5 mm	0.5x0.5 mm	C2-C3	Jim 7.0/Semi, ASM (Horsfield et al., 2010)
David et al., 2022	3 T	Siemens SkyraFit	T2*-3D MEDIC	2.5 mm	0.5x0.5 mm	C2/C3	Jim 7.0/Semi, ASM (Horsfield et al., 2010)
Ellingson et al., 2008	1.5 T	GE Horizon	DTI	5 mm	1.56x1.56 mm	C1-C4	Manual, template
Freund et al., 2011b	1.5 T	Siemens Magnetom Sonata	T1-3D MDEFT	3 mm	1x1mm	C2	Dispimage/Semi, Losseff (Losseff et al., 1996)
Freund et al., 2013	3 T	Siemens Magnetom Verio	T1-3D MPRAGE	3 mm	1x1mm	C2/C3	Jim 6.0/Semi, ASM (Horsfield et al., 2010) & Losseff (Losseff et al., 1996)
Grabher et al., 2015	3 T	Siemens Magnetom Verio	T1-3D MPRAGE	3 mm	1x1mm	C2/C3	Jim 6.0/Semi, ASM (Horsfield et al., 2010)
Hou et al., 2014	3 T	Siemens TIM Trio	T1-3D MPRAGE	1 mm	1x1mm	C2	Semi, Losseff (Losseff et al., 1996)
Hou et al., 2016	3 T	Siemens TIM Trio	T1-3D MPRAGE	1 mm	1x1mm	C2	Semi, Losseff (Losseff et al., 1996)
Hug et al., 2021	3 T	Siemens Magnetom Verio	T1	1 mm	1x1mm	C2/C3	Snap-ITK/Manual
Jutzeler et al., 2016	3 T	Philips Ingenia	T1 3D-GRE	1 mm	1x1mm	C2	Semi
Kikkert et al., 2021	3 T	Philips Ingenia	T2	2 mm	1x1mm	C2/C3	Jim 7.0/Semi, ASM (Horsfield et al., 2010) & Losseff (Losseff et al., 1996)
Lundell et al., 2011	3 T	Siemens Trio	T1 MPRAGE	1 mm	1x1mm	C2	Semi, Losseff (Losseff et al., 1996)
Mesbah et al., 2021	3 T	Siemens Magnetom Skyra	T2	3 mm	0.35x0.35	C3	Manual
Ohn et al., 2013	3 T	Philips Achieva	DTI	3 mm	1.25x1.5 mm	C2-C7	MedINRIA 1.6/Manual
Pfyffer et al., 2020	3 T	Philips Achieva	T2	3.2 mm	0.5x0.5 mm	C2/C3	Jim 7.0/Semi, ASM (Horsfield et al., 2010)
Sangari et al., 2019	3 T	Siemens TIM Trio	T2	3 mm	0.6x0.6 mm	C2	Semi, Losseff (Losseff et al., 1996)
Schmit and Cole, 2004	1.5 T	GE Horizon	T2 FLAIR	5 mm	0.625 × 0.625 mm	C3	Semi
Seif et al., 2018	3 T	Siemens Magnetom SkyraFit and Verio	T1-3D MPRAGE	1 mm	1x1mm	C2/C3	Jim 7.0/Semi, ASM
Seif et al., 2020	3 T	Siemens Magnetom SkyraFit	T2*-3D MEDIC	2.5 mm	0.25x0.25 mm	C2/C3	Jim 6.0/Semi, ASM (Horsfield et al., 2010)
Wyss et al., 2019	3 T	Philips Achieva	T2	3.2 mm	0.5x0.5 mm	C2	Jim 6.0/Semi, ASM (Horsfield et al., 2010)
Ziegler et al., 2018	3 T	Siemens Magnetom SkyraFit and Verio	T1-3D MPRAGE	1 mm	1x1mm	C2/C3	Jim 6.0/Semi, ASM

Imaging parameters of included studies. The image analysis column denotes software used to extract cross-sectional cervical spinal cord area (cSC CSA) (if specified) and type of cSC CSA-extraction method. Auto = automated cSC CSA extraction. Semi = semiautomated cSC CSA extraction. Manual = manual cSC CSA extraction. ASM = active surface method.

(Azzarito et al., 2020).

Only one article investigated spasticity and cSC CSA, in which a moderate correlation was found (Pearson's r = 0.57). cSC CSA was further reduced in non-spastic than in spastic PwSCI (Sangari et al., 2019).

Results on association between cSC CSA and sensorimotor function are differing. Although SCIM and upper and lower extremity strength improved over time, one longitudinal study (David et al., 2021) did not find any correlation between baseline cSC CSA and 1.5-year outcome scores. Another longitudinal study investigating partly the same cohort as (Freund et al., 2013) found, however, that PwSCI with smaller cSC CSA had worse pinprick-score whereas PwSCI with less decrease in cSC CSA had better lower extremity strength at two years follow-up (Ziegler et al., 2018). In addition, larger cSC CSA has been associated with better motor score or motor recovery as reported in three studies (Cohen-Adad et al., 2011; Hou et al., 2016; Lundell et al., 2011). PwSCI with larger cSC CSA had better sensory function in three studies (Azzarito et al., 2020; Cohen-Adad et al., 2011; Lundell et al., 2011), with one of these studies (Azzarito et al., 2020) however only finding an association between cSC CSA - pinprick score and not cSC CSA - light touch. Further, pinprick scores at 12 months were associated with rate of cord area decrease (Grabher et al., 2015). On the contrary and similar to findings from a longitudinal cohort (David et al., 2021), two studies (Hou et al., 2014; Jutzeler et al., 2016) did not find any relationship between sensory function, motor score and cSC CSA apart from increased warm perception thresholds in PwSCI with smaller cSC CSA (Jutzeler et al., 2016). One study did not find any association between cSC CSA – motor score (Azzarito et al., 2020).

4. Discussion

This article characterizes the effects of spinal cord injury on cervical spinal cord atrophy. In accordance with previous studies, cSC CSA is reduced following SCI. The atrophy corresponds to a SMD of −1.48 (95% CI −1.78 to −1.19; mean difference −13.5 mm^2; 95% CI −16.6 to −10.5 mm^2). Spinal cord atrophy with decreased cSC CSA is not unique to spinal cord injuries and has been well described following multiple sclerosis (MS) (Casserly et al., 2018) (-8 mm^2 cSC CSA for all MS-subtypes versus controls) and degenerative cervical myelopathy (David et al., 2022; Seif et al., 2020) (−24 to −13 mm^2 cSC CSA versus

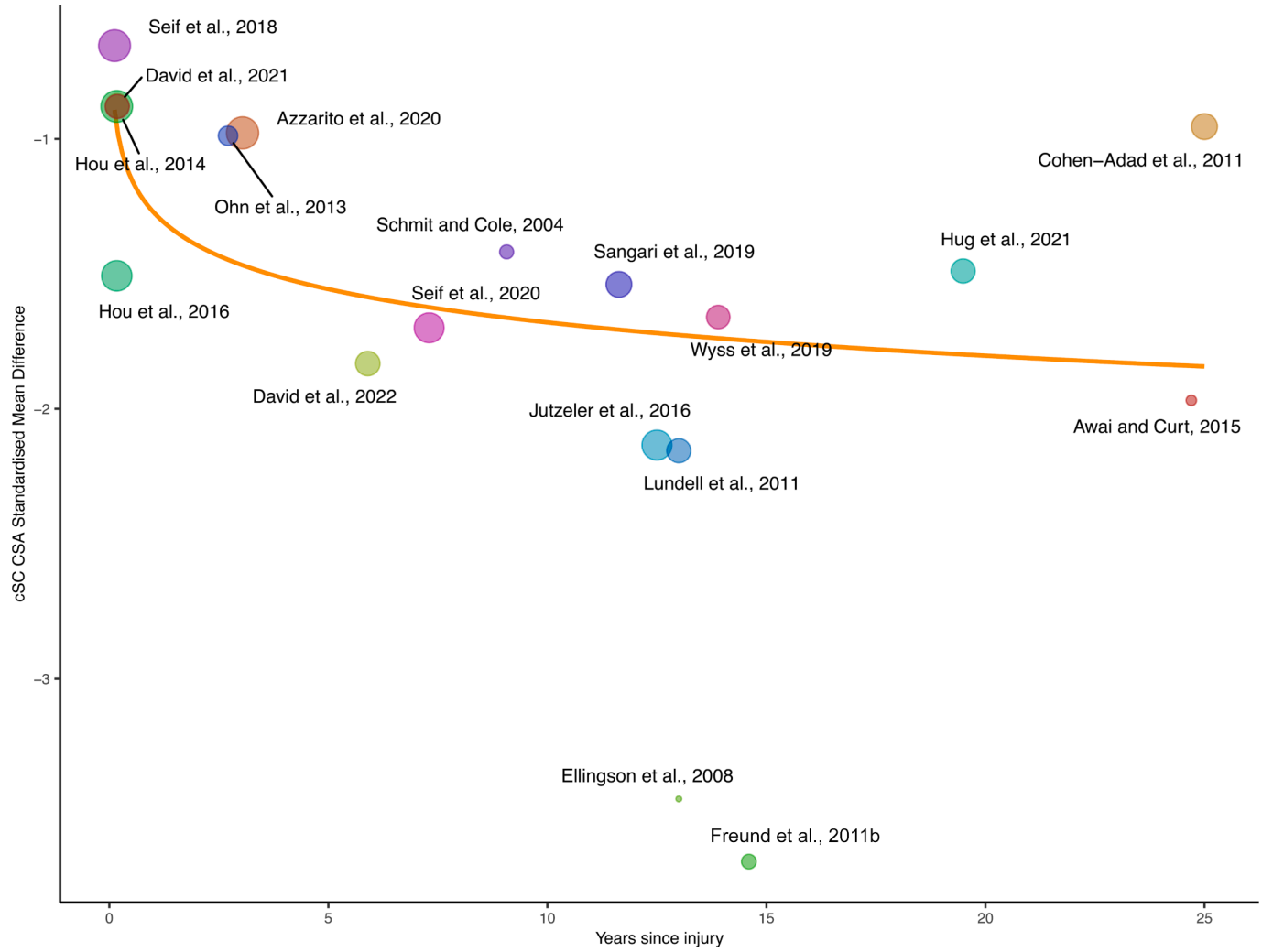

Fig. 4. Meta-regression for studies included in cervical spinal cord cross-sectional area (cSC CSA) atrophy meta-analysis. Natural logarithm time since injury (lnTSI) is used as a moderator. The model has the following statistics: $\tau^2 = 0.08$, $\tau = 0.3$, $I^2 = 31.4\%$, $H^2 = 1.46$, $R^2 = 60.7\%$. Point sizes are corresponding to study weights. cSC CSA standardized mean difference = −1.27 – (0.178*ln(years after injury)), p = 0.0035.

controls). The longitudinal atrophy was best described using a natural logarithmic model. Women with SCI were underrepresented compared to female controls; as cSC CSA tends to be lower in females (Solstrand Dahlberg et al., 2020), the effect sizes may thus be larger than those observed here.

Although moderate-to-substantial heterogeneity was suggested in the cSC CSA atrophy meta-analysis, no study reported a larger cSC CSA in PwSCI than in controls. Thus, the findings should be considered robust despite the heterogeneity as the meta-analytical evidence clearly indicated atrophy. It should be noted that spinal cord injuries and PwSCI are heterogenous, which is possibly reflected in the reported values. Additional heterogeneity can be introduced with different TSI, scanning regimens and/or image analysis paradigms.

As shown by the meta-regression, lnTSI influences heterogeneity. This finding most likely reflects a change in cord atrophy dynamics over time, consistent with longitudinal studies, where atrophy first occurs at a rapid rate but eventually decreases over time (Ziegler et al., 2018). The meta-regression findings were further consistent with results from the longitudinal subgroup study where the lnTSI-model had a better fit than the linear TSI-model.

Despite progressing cord atrophy, SCIM-scores improve (David et al., 2021; Freund et al., 2013; Ziegler et al., 2018). The paradox between decrease in cSC CSA (or increased atrophy) and the improvement in function, as measured through SCIM, further sheds light on the difficulties in correlating imaging metrics with more complex functional measurements. Another example of this are findings where sex, brain volume and body length, but not motor behaviors, were predictors of cSC CSA in 283 young healthy adults (Solstrand Dahlberg et al., 2020). Although motor and sensory function after spinal injury may or may not improve (as measured with the ISNCSCI assessment), the ability to use remaining function in activity can improve through, for example, training or the use of aids.

Due to data availability, more than a third of the data points (37.5%) included in the regression model had a TSI of two years or less which may decrease the generalizability and overall predictability of the model. While the included population was generally reflective of the sex distribution in SCI, women with SCI were underrepresented compared to women controls. The re-use of data and/or study participants is understandable given potential difficulties in recruitment, and clear reporting of re-use would facilitate meta-analytical work. To increase the available data points, manual data extraction was performed in some of the studies which may have introduced additional bias.

Half of the studies in the meta-analysis (Awai and Curt, 2015; Azzarito et al., 2020; David et al., 2022, 2021; Freund et al., 2011b; Jutzeler et al., 2016; Seif et al., 2020, 2018; Wyss et al., 2019) and 6/8 of the studies in the meta-correlation were published by the same group (Azzarito et al., 2020; David et al., 2021; Freund et al., 2013, 2011b; Jutzeler et al., 2016; Pfyffer et al., 2020). While the quality of this work

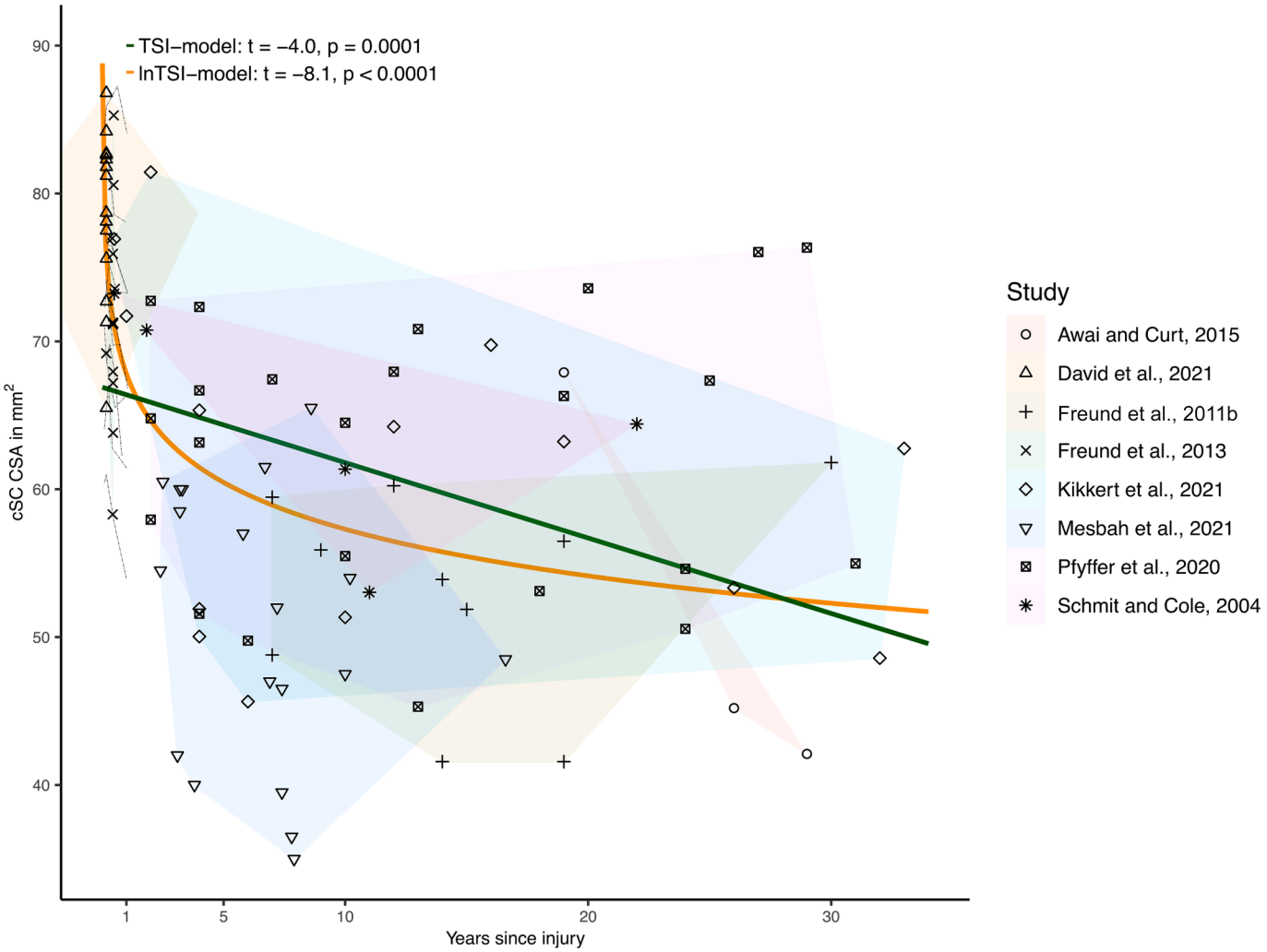

Fig. 5. Longitudinal models depicting cervical spinal cord atrophy over time in individual persons with spinal cord injury (PwSCI). PwsCI from the respective studies are labelled based on study. Data points from respective study are encircled in differently colored fields. Note that averaged individual time since injury and cervical spinal cord cross-sectional area (cSC CSA) values are used for PwSCI from one longitudinal study (Freund et al., 2013). The individual longitudinal trajectories from this study are visualized with dashed black lines, but not included in the two statistical models. The equations for the respective models are cSC CSA = 67.8 – (4.56*ln (years after injury)) and cSC CSA = 66.9 – (0.51*years after injury).

is excellent (and here we strived to only include unique individuals), this circumstance may have introduced additional bias and could warrant caution when interpreting the current results. Additional groups engaging in spinal cord injury neuroimaging would corroborate the field.

A limitation to the use of cSC CSA as a marker of atrophy is that with cervical lesions, cSC CSA at C2/C3 may be influenced by both local and distal degeneration mechanisms, as neurodegeneration is greater near the lesion. An alternative may be to investigate cord properties at the lumbar enlargement (David et al., 2019), where infralesional atrophy after SCI is also evident, or, ideally, to assess atrophy profiles along the entire cord using high resolution structural and diffusion imaging. Additionally, lesions close to the C2/C3 level may introduce other aspects, including direct tissue loss due to injury proximity, see for example (Kikkert et al., 2021).

Spinal cord atrophy has been linked to other neuroimaging metrics, such as metabolite profile (Pfyffer et al., 2020; Wyss et al., 2019), diffusion properties (Cohen-Adad et al., 2011; Ellingson et al., 2008), and more detailed specifications of tract alterations within the spinal cord (David et al., 2021). While beyond the current scope, such modalities and further development of spinal cord neuroimaging methods, including functional MRI and PET, will continue to contribute to better understanding the mechanisms behind post-SCI spinal atrophy.

In conclusion, there is significant spinal cord atrophy after SCI, and atrophy may be more severe in more rostral lesions. The rate of atrophy is highest immediately after injury but slows over time. To improve prognostic precision and coherency between studies, further standardization in imaging protocols and imaging analysis is desirable and has been proposed (Cohen-Adad et al., 2021). Due to the nature of atrophy following SCI and to avoid confounders, future studies investigating cord imaging metrics would ideally include PwSCI at similar time points after injury and/or utilize a longitudinal design.

Longitudinal studies with acute as well as early imaging time-points (<1 month after injury) could further help characterize the onset of remote atrophy. At the other end of the spectrum, longitudinal development of cSC CSA beyond three years since injury remains to be investigated. These logistically challenging studies have proven to be extremely valuable in characterizing the time course of SCI-induced cord atrophy and may inform on the efficacy of early interventions.

Further, as sex influences cSC CSA, sex-matched controls should be preferred. Given increases in women with SCI, new studies should strive to obtain representative samples (Moschovou et al., 2022). Due to the relative sparsity of PwSCI, data sharing within the SCI-imaging community could enable more robust modelling. The magnitude and

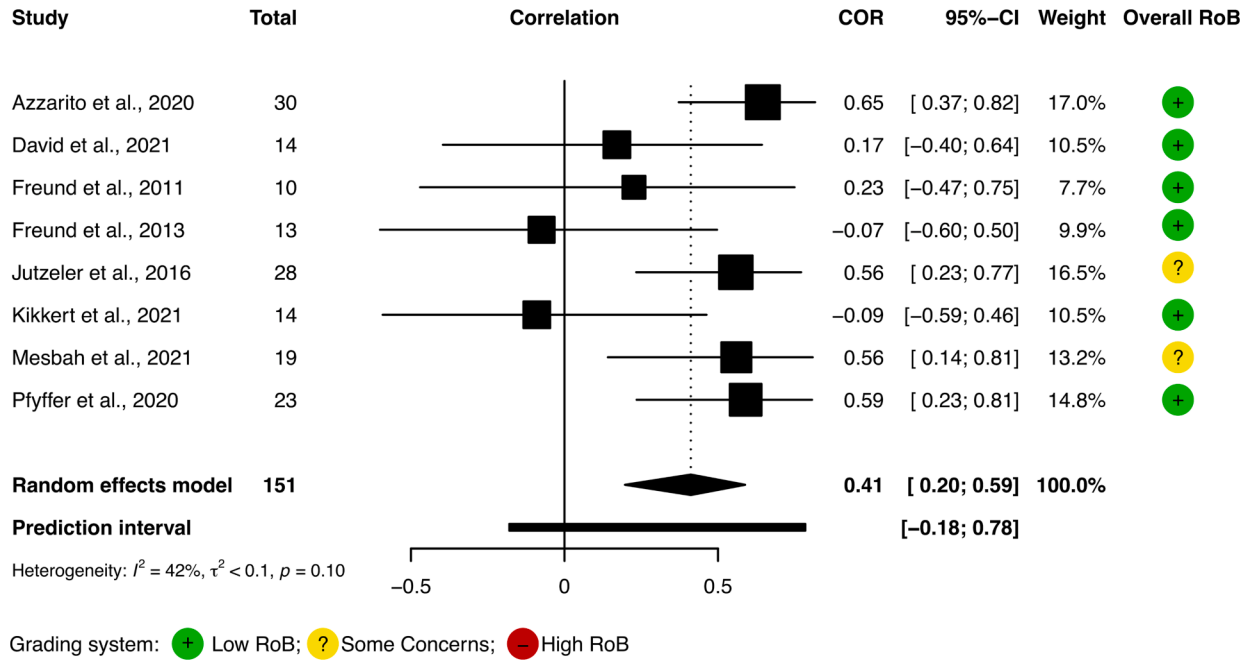

Fig. 6. Meta-correlation Forest plot. A modest correlation between level of injury and cervical spinal cord cross-sectional area is depicted.

consistency of reductions in cSC CSA after spinal cord injury indicate that supra-lesional cord atrophy is an important marker. If the magnitude of cSC CSA loss can be limited by acute care or rehabilitation interventions remains to be investigated.

Funding

This study was funded by the Promobilia Foundation (2013-H1 and 2015-H2); Wings for Life (WFL-US-014/14); the Department of Defense (CDMRP SC140194); and the National Institutes of Health (5R01HD097407).

Data availability

Study data is available from the authors upon reasonable request. Sharing of raw data obtained through personal correspondence is contingent on original author permission.

Declaration of Competing Interest

The authors declare that they have no known competing financial interests or personal relationships that could have appeared to influence the work reported in this paper.

Data availability

Study data is available from the authors upon reasonable request. Sharing of raw data obtained through personal correspondence is contingent on original author permission.

Acknowledgements

The authors would like to thank all the contacted study authors who helpfully and kindly responded to our inquiries.

References

Awai, L., Curt, A., 2015. Preserved sensory-motor function despite large-scale morphological alterations in a series of patients with holocord syringomyelia. J. Neurotrauma 32, 403–410. https://doi.org/10.1089/neu.2014.3536.

Azzarito, M., Seif, M., Kyathanahally, S., Curt, A., Freund, P., 2020. Tracking the neurodegenerative gradient after spinal cord injury. NeuroImage Clin. 26, 102221 https://doi.org/10.1016/j.nicl.2020.102221.

Azzarito, M., Kyathanahally, S.P., Balbastre, Y., Seif, M., Blaiotta, C., Callaghan, M.F., Ashburner, J., Freund, P., 2021. Simultaneous voxel-wise analysis of brain and spinal cord morphometry and microstructure within the SPM framework. Hum. Brain Mapp. 42, 220–232. https://doi.org/10.1002/hbm.25218.

Balduzzi, S., Rücker, G., Schwarzer, G., 2019. How to perform a meta-analysis with R: a practical tutorial. Evid. Based Ment. Health 22, 153–160. https://doi.org/10.1136/ebmental-2019-300117.

Casserly, C., Seyman, E.E., Alcaide-Leon, P., Guenette, M., Lyons, C., Sankar, S., Svendrovski, A., Baral, S., Oh, J., 2018. Spinal Cord Atrophy in Multiple Sclerosis: A Systematic Review and Meta-Analysis. J. Neuroimaging Off. J. Am. Soc. Neuroimaging 28, 556–586. https://doi.org/10.1111/jon.12553.

Cohen-Adad, J., El Mendili, M.-M., Lehéricy, S., Pradat, P.-F., Blancho, S., Rossignol, S., Benali, H., 2011. Demyelination and degeneration in the injured human spinal cord detected with diffusion and magnetization transfer MRI. NeuroImage 55, 1024–1033. https://doi.org/10.1016/j.neuroimage.2010.11.089.

Cohen-Adad, J., Alonso-Ortiz, E., Abramovic, M., Arneitz, C., Atcheson, N., Barlow, L., Barry, R.L., Barth, M., Battiston, M., Büchel, C., Budde, M., Callot, V., Combes, A.J. E., De Leener, B., Descoteaux, M., de Sousa, P.L., Dostál, M., Doyon, J., Dvorak, A., Eippert, F., Epperson, K.R., Epperson, K.S., Freund, P., Finsterbusch, J., Foias, A., Fratini, M., Fukunaga, I., Wheeler-Kingshott, C.A.M.G., Germani, G., Gilbert, G., Giove, F., Gros, C., Grussu, F., Hagiwara, A., Henry, P.-G., Horák, T., Hori, M., Joers, J., Kamiya, K., Karbasforoushan, H., Keřkovský, M., Khatibi, A., Kim, J.-W., Kinany, N., Kitzler, H., Kolind, S., Kong, Y., Kudlička, P., Kuntke, P., Kurniawan, N. D., Kusmia, S., Labounek, R., Laganà, M.M., Laule, C., Law, C.S., Lenglet, C., Leutritz, T., Liu, Y., Llufriu, S., Mackey, S., Martinez-Heras, E., Mattera, L., Nestrasil, I., O'Grady, K.P., Papinutto, N., Papp, D., Pareto, D., Parrish, T.B., Pichiecchio, A., Prados, F., Rovira, À., Ruitenberg, M.J., Samson, R.S., Savini, G., Seif, M., Seifert, A.C., Smith, A.K., Smith, S.A., Smith, Z.A., Solana, E., Suzuki, Y., Tackley, G., Tinnermann, A., Valošek, J., Van De Ville, D., Yiannakas, M.C., Weber, K.A., Weiskopf, N., Wise, R.G., Wyss, P.O., Xu, J., 2021. Generic acquisition protocol for quantitative MRI of the spinal cord. Nat. Protoc. 16, 4611–4632. https://doi.org/10.1038/s41596-021-00588-0.

David, G., Seif, M., Huber, E., Hupp, M., Rosner, J., Dietz, V., Weiskopf, N., Mohammadi, S., Freund, P., 2019. In vivo evidence of remote neural degeneration in the lumbar enlargement after cervical injury. Neurology 92, e1367–e1377. https://doi.org/10.1212/WNL.0000000000007137.

David, G., Pfyffer, D., Vallotton, K., Pfender, N., Thompson, A., Weiskopf, N., Mohammadi, S., Curt, A., Freund, P., 2021. Longitudinal changes of spinal cord grey and white matter following spinal cord injury. J. Neurol. Neurosurg. Psychiatry 92, 1222–1230. https://doi.org/10.1136/jnnp-2021-326337.

David, G., Vallotton, K., Hupp, M., Curt, A., Freund, P., Seif, M., 2022. Extent of Cord Pathology in the Lumbosacral Enlargement in Non-Traumatic versus Traumatic Spinal Cord Injury. J. Neurotrauma 39, 639–650. https://doi.org/10.1089/neu.2021.0389.

Ellingson, B.M., Ulmer, J.L., Schmit, B.D., 2008. Morphology and morphometry of human chronic spinal cord injury using diffusion tensor imaging and fuzzy logic. Ann. Biomed. Eng. 36, 224–236. https://doi.org/10.1007/s10439-007-9415-6.

Freund, P., Dalton, C., Wheeler-Kingshott, C.A.M., Glensman, J., Bradbury, D., Thompson, A.J., Weiskopf, N., 2010. Method for simultaneous voxel-based morphometry of the brain and cervical spinal cord area measurements using 3D-MDEFT. J. Magn. Reson. Imaging JMRI 32, 1242–1247. https://doi.org/10.1002/jmri.22340.

Freund, P., Rothwell, J., Craggs, M., Thompson, A.J., Bestmann, S., 2011a. Corticomotor representation to a human forearm muscle changes following cervical spinal cord injury. Eur. J. Neurosci. 34, 1839–1846. https://doi.org/10.1111/j.1460-9568.2011.07895.x.

Freund, P., Weiskopf, N., Ward, N.S., Hutton, C., Gall, A., Ciccarelli, O., Craggs, M., Friston, K., Thompson, A.J., 2011b. Disability, atrophy and cortical reorganization following spinal cord injury. Brain J. Neurol. 134, 1610–1622. https://doi.org/10.1093/brain/awr093.

Freund, P., Schneider, T., Nagy, Z., Hutton, C., Weiskopf, N., Friston, K., Wheeler-Kingshott, C.A., Thompson, A.J., 2012a. Degeneration of the injured cervical cord is associated with remote changes in corticospinal tract integrity and upper limb impairment. PloS One 7, e51729.

Freund, P., Wheeler-Kingshott, C.A., Nagy, Z., Gorgoraptis, N., Weiskopf, N., Friston, K., Thompson, A.J., Hutton, C., 2012b. Axonal integrity predicts cortical reorganisation following cervical injury. J. Neurol. Neurosurg. Psychiatry 83, 629–637. https://doi.org/10.1136/jnnp-2011-301875.

Freund, P., Weiskopf, N., Ashburner, J., Wolf, K., Sutter, R., Altmann, D.R., Friston, K., Thompson, A., Curt, A., 2013. MRI investigation of the sensorimotor cortex and the corticospinal tract after acute spinal cord injury: a prospective longitudinal study. Lancet Neurol. 12, 873–881. https://doi.org/10.1016/S1474-4422(13)70146-7.

Grabher, P., Callaghan, M.F., Ashburner, J., Weiskopf, N., Thompson, A.J., Curt, A., Freund, P., 2015. Tracking sensory system atrophy and outcome prediction in spinal cord injury. Ann. Neurol. 78, 751–761. https://doi.org/10.1002/ana.24508.

Harrer, M., Cuijpers, P., Furukawa, T.A., Ebert, D.D., 2021. Doing Meta-Analysis with R: A Hands-On Guide. Chapman & Hall/CRC Press, Boca Raton, FL and London.

Horsfield, M.A., Sala, S., Neema, M., Absinta, M., Bakshi, A., Sormani, M.P., Rocca, M.A., Bakshi, R., Filippi, M., 2010. Rapid semi-automatic segmentation of the spinal cord from magnetic resonance images: application in multiple sclerosis. NeuroImage 50, 446–455. https://doi.org/10.1016/j.neuroimage.2009.12.121.

Hou, J., Xiang, Z., Yan, R., Zhao, M., Wu, Y., Zhong, J., Guo, L., Li, H., Wang, J., Wu, J., Sun, T., Liu, H., 2016. Motor recovery at 6 months after admission is related to structural and functional reorganization of the spine and brain in patients with spinal cord injury. Hum. Brain Mapp. 37, 2195–2209. https://doi.org/10.1002/hbm.23163.

Hou, J.-M., Yan, R.-B., Xiang, Z.-M., Zhang, H., Liu, J., Wu, Y.-T., Zhao, M., Pan, Q.-Y., Song, L.-H., Zhang, W., Li, H.-T., Liu, H.-L., Sun, T.-S., 2014. Brain sensorimotor system atrophy during the early stage of spinal cord injury in humans. Neuroscience 266, 208–215. https://doi.org/10.1016/j.neuroscience.2014.02.013.

Huber, E., David, G., Thompson, A.J., Weiskopf, N., Mohammadi, S., Freund, P., 2018. Dorsal and ventral horn atrophy is associated with clinical outcome after spinal cord injury. Neurology 90, e1510–e1522. https://doi.org/10.1212/WNL.0000000000005361.

Hug, A., Bernini, A., Wang, H., Lutti, A., Jende, J.M.E., Böttinger, M., Weber, M.-A., Weidner, N., Lang, S., 2021. In chronic complete spinal cord injury supraspinal changes detected by quantitative MRI are confined to volume reduction in the caudal brainstem. NeuroImage Clin. 31, 102716 https://doi.org/10.1016/j.nicl.2021.102716.

Jutzeler, C.R., Huber, E., Callaghan, M.F., Luechinger, R., Curt, A., Kramer, J.L.K., Freund, P., 2016. Association of pain and CNS structural changes after spinal cord injury. Sci. Rep. 6, 18534. https://doi.org/10.1038/srep18534.

Kassambara, A., 2020. ggpubr: "ggplot2" Based Publication Ready Plots.

Kikkert, S., Pfyffer, D., Verling, M., Freund, P., Wenderoth, N., 2021. Finger somatotopy is preserved after tetraplegia but deteriorates over time. eLife 10, e67713.

Losseff, N.A., Webb, S.L., O'Riordan, J.I., Page, R., Wang, L., Barker, G.J., Tofts, P.S., McDonald, W.I., Miller, D.H., Thompson, A.J., 1996. Spinal cord atrophy and disability in multiple sclerosis. A new reproducible and sensitive MRI method with potential to monitor disease progression. Brain J. Neurol. 119 (Pt 3), 701–708. https://doi.org/10.1093/brain/119.3.701.

Lundell, H., Barthelemy, D., Skimminge, A., Dyrby, T.B., Biering-Sørensen, F., Nielsen, J. B., 2011. Independent spinal cord atrophy measures correlate to motor and sensory deficits in individuals with spinal cord injury. Spinal Cord 49, 70–75. https://doi.org/10.1038/sc.2010.87.

Mesbah, S., Ball, T., Angeli, C., Rejc, E., Dietz, N., Ugiliweneza, B., Harkema, S., Boakye, M., 2021. Predictors of volitional motor recovery with epidural stimulation in individuals with chronic spinal cord injury. Brain J. Neurol. 144, 420–433. https://doi.org/10.1093/brain/awaa423.

Moschovou, M., Antepohl, W., Halvorsen, A., Pettersen, A.L., Divanoglou, A., 2022. Temporal changes in demographic and injury characteristics of traumatic spinal cord injuries in Nordic countries – a systematic review with meta-analysis. Spinal Cord 60, 765–773. https://doi.org/10.1038/s41393-022-00772-3.

Ohn, S.H., Kim, D.Y., Shin, J.C., Kim, S.M., Yoo, W.-K., Lee, S.-K., Park, C.-H., Jung, K.-I., Jang, K.U., Seo, C.H., Koh, S.H., Jung, B., 2013. Analysis of high-voltage electrical spinal cord injury using diffusion tensor imaging. J. Neurol. 260, 2876–2883. https://doi.org/10.1007/s00415-013-7081-1.

Oyinbo, C.A., 2011. Secondary injury mechanisms in traumatic spinal cord injury: a nugget of this multiply cascade. Acta Neurobiol. Exp. (Warsz.) 71, 281–299.

Page, M.J., McKenzie, J.E., Bossuyt, P.M., Boutron, I., Hoffmann, T.C., Mulrow, C.D., Shamseer, L., Tetzlaff, J.M., Akl, E.A., Brennan, S.E., Chou, R., Glanville, J., Grimshaw, J.M., Hróbjartsson, A., Lalu, M.M., Li, T., Loder, E.W., Mayo-Wilson, E., McDonald, S., McGuinness, L.A., Stewart, L.A., Thomas, J., Tricco, A.C., Welch, V.A., Whiting, P., Moher, D., 2021. The PRISMA 2020 statement: an updated guideline for reporting systematic reviews. BMJ 372, n71. https://doi.org/10.1136/bmj.n71.

Papinutto, N., Schlaeger, R., Panara, V., Zhu, A.H., Caverzasi, E., Stern, W.A., Hauser, S. L., Henry, R.G., 2015. Age, gender and normalization covariates for spinal cord gray matter and total cross-sectional areas at cervical and thoracic levels: a 2D phase sensitive inversion recovery imaging study. PloS One 10, e0118576.

Pfyffer, D., Wyss, P.O., Huber, E., Curt, A., Henning, A., Freund, P., 2020. Metabolites of neuroinflammation relate to neuropathic pain after spinal cord injury. Neurology 95, e805–e814. https://doi.org/10.1212/WNL.0000000000010003.

R Core Team, 2021. R: A Language and Environment for Statistical Computing.

Rohatgi, A., 2021. WebPlotDigitizer.

RStudio Team, 2021. RStudio: Integrated Development Environment for R.

Rudis, B., Bolker, B., Schulz, J., 2017. ggalt: Extra Coordinate Systems, "Geoms", Statistical Transformations, Scales and Fonts for "ggplot2.".

Rüegg, T.B., Wicki, A.G., Aebli, N., Wisianowsky, C., Krebs, J., 2015. The diagnostic value of magnetic resonance imaging measurements for assessing cervical spinal canal stenosis. J. Neurosurg. Spine 22, 230–236. https://doi.org/10.3171/2014.10.SPINE14346.

Sangari, S., Lundell, H., Kirshblum, S., Perez, M.A., 2019. Residual descending motor pathways influence spasticity after spinal cord injury. Ann. Neurol. 86, 28–41. https://doi.org/10.1002/ana.25505.

Schmit, B.D., Cole, M.K., 2004. Quantification of morphological changes in the spinal cord in chronic spinal cord injury using magnetic resonance imaging. Conf. Proc. Annu. Int. Conf. IEEE Eng. Med. Biol. Soc. IEEE Eng. Med. Biol. Soc. Annu. Conf. 2004, 4425–4428. 10.1109/IEMBS.2004.1404230.

Seif, M., Curt, A., Thompson, A.J., Grabher, P., Weiskopf, N., Freund, P., 2018. Quantitative MRI of rostral spinal cord and brain regions is predictive of functional recovery in acute spinal cord injury. NeuroImage Clin. 20, 556–563. https://doi.org/10.1016/j.nicl.2018.08.026.

Seif, M., David, G., Huber, E., Vallotton, K., Curt, A., Freund, P., 2020. Cervical cord neurodegeneration in traumatic and non-traumatic spinal cord injury. J. Neurotrauma 37, 860–867. https://doi.org/10.1089/neu.2019.6694.

Sheshkin, D., J., 2000. Measures of Association/Correlation, Test 29. Spearman's Rank-Order Correlation Coefficient, VI. 5. Use of Fisher's zr transformation with Spearman's rank-order correlation coefficient. In: Handbook of Parametric and Nonparametric Statistical Procedures. Chapman & Hall/CRC, Boca Raton, FL, p. 880.

Slowikowski, K., 2021. ggrepel: Automatically Position Non-Overlapping Text Labels with "ggplot2.".

Solstrand Dahlberg, L., Viessmann, O., Linnman, C., 2020. Heritability of cervical spinal cord structure. Neurol. Genet. 6, e401.

Song, K.-J., Choi, B.-W., Kim, S.-J., Kim, G.-H., Kim, Y.-S., Song, J.-H., 2009. The relationship between spinal stenosis and neurological outcome in traumatic cervical spine injury: an analysis using Pavlov's ratio, spinal cord area, and spinal canal area. Clin. Orthop. Surg. 1, 11–18. https://doi.org/10.4055/cios.2009.1.1.11.

The American Spinal Injury Association, 2019. International Standards for Neurological Classification of SCI (ISNCSCI) Worksheet.

Van Broeckhoven, J., Sommer, D., Dooley, D., Hendrix, S., Franssen, A.J.P.M., 2021. Macrophage phagocytosis after spinal cord injury: when friends become foes. Brain J. Neurol. 144, 2933–2945. https://doi.org/10.1093/brain/awab250.

Viechtbauer, W., 2005. Bias and efficiency of meta-analytic variance estimators in the random-effects model. J. Educ. Behav. Stat. 30, 261–293.

Wickham, H., Bryan, J., 2019. readxl: Read Excel Files.

Wickham, H., 2016. ggplot2: Elegant Graphics for Data Analysis.

Wyss, P.O., Huber, E., Curt, A., Kollias, S., Freund, P., Henning, A., 2019. MR spectroscopy of the cervical spinal cord in chronic spinal cord injury. Radiology 291, 131–138. https://doi.org/10.1148/radiol.2018181037.

Ziegler, G., Grabher, P., Thompson, A., Altmann, D., Hupp, M., Ashburner, J., Friston, K., Weiskopf, N., Curt, A., Freund, P., 2018. Progressive neurodegeneration following spinal cord injury: Implications for clinical trials. Neurology 90, e1257–e1266. https://doi.org/10.1212/WNL.0000000000005258.